

Casting of Lead-free Solder Bulk Specimens With Various Solidification Rates

J. Madeni*, S. Liu*, T. Siewert**

*Center for Welding, Joining and Coatings Research
George S. Ansell Department of Metallurgical & Materials Engineering
Colorado School of Mines
Golden, Colorado 80401, U.S.A.

**Materials Reliability Division
National Institute of Standards and Technology
Boulder, Colorado 80305, U.S.A.

ABSTRACT

The casting of lead-free solder bulk samples has been investigated by varying the conditions of solidification. Two sets of samples were generated, one water-quenched and the other air-cooled. From these cast samples, tensile testing specimens were produced for the investigation of their mechanical properties. Cooling rate effects were specifically analyzed using small solder droplets. Excellent correlations between secondary dendrite arm spacings, microhardness measurements and tensile properties with the cooling rates were found. The results indicated that samples produced in accordance with the recommendations of the National Center for Manufacturing Sciences exhibited coarser microstructures (indicative of slower cooling) than the microstructures of actual solder joints (indicative of faster cooling). Based on this study, the predicted performance (lifetime and reliability) of actual soldering joints will not compare well with that of actual solder joints.

INTRODUCTION

This research is of significant interest to the electronics industry. As is well known, lead-based solder materials are a critical part of the packaging in the electronic materials technology. However, because lead is detrimental to the well-being of humans and the environment, there is a considerable interest in the development of alternate lead-free soldering materials with similar or improved properties.

Generally, solder joints are subjected to thermal cycles during operation [1]. During the thermal cycles, thermal stresses and strains develop and thus generate distortions of the joint. The extent of these distortions is strongly controlled by the value of the coefficient of thermal expansion of the components as well as the difference of temperature between them. Figure 1 is a

schematic illustration of a typical solder joint connecting a surface mount component (SMC) to a printed circuit board (PCB) at an initial temperature, T_0 , and the same solder joint at a higher temperature T_1 . Note the appearance of stresses and strains within the joint caused by the temperature change. If the mechanical properties of the solder alloy are known, these values can be used in mathematical modeling to predict the reliability and lifetime of the solder joint. In the case of newly developed materials, tensile and fatigue data first need to be collected before suitable models for joint reliability can be developed.

A National Electronics Manufacturing Initiative (NEMI) task group has identified nearly a hundred candidate solder alloys for testing and evaluation. The present work deals with the analysis of three of these alloys.

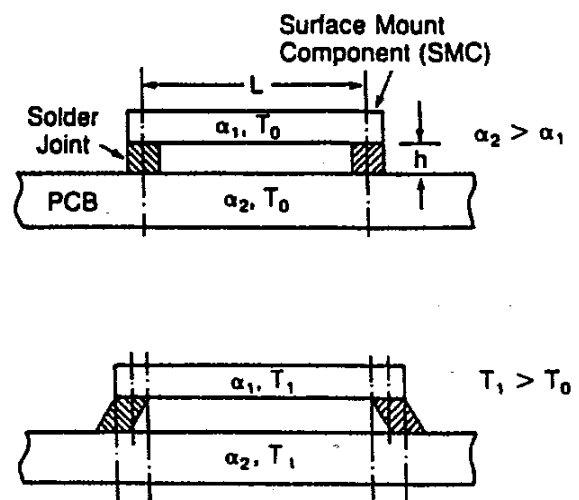


Figure 1. Representation of the distortions occurring in a solder joint resulting from thermal cycling [1].

SCOPE OF THE RESEARCH

Three lead-free solder alloys were selected for a detailed investigation. They were fabricated based upon two binary and one ternary eutectic system. These low-melting point alloys are the following:

- a) Sn-3.5Ag with $T_m = 221^\circ\text{C}$
- b) Sn-0.7Cu with $T_m = 227^\circ\text{C}$, and
- c) Sn-3.2Ag-0.8Cu with $T_m = 217^\circ\text{C}$

This study includes the generation of cast bulk samples for the production of tensile test specimens at two different solidification rates, one set of samples was water-quenched and the other set was air-cooled. Mechanical properties were measured from tensile tests and hardness testing.

However, after observing similarities between the tensile properties of the specimens produced at the two solidification rates, solder droplets with three different cooling rates were produced for comparison. The microstructure was characterized using light microscopy, scanning electron microscopy (SEM) and energy dispersive spectroscopy (EDS). Additionally, microhardness was measured throughout the solidification microstructure to determine possible correlation with the mechanical properties.

EXPERIMENTAL PART

Casting of Bulk Specimens

The bulk specimens were cast inside a cylindrical mold made of titanium, which was preheated to 150°C above the melting points of the alloys. The mold was 5-inches tall (12.7 cm.) with an internal radius of 1/4 inches (0.635 cm.) and an external radius of 7/32 inches (0.556 cm.). The resulting wall thickness of 0.03 inches (0.0762 cm) was thin enough compared to the internal volume of the mold to promote an efficient heat extraction during quenching.

The solder alloys were melted and maintained 100°C above their respective melting point for 20 minutes in an argon atmosphere. A first set of specimens was quenched (Q) into water. The measured water temperature was 14°C . All of these steps were in accordance with recommendations from the National Center for Manufacturing Sciences (NCMS) [2].

For comparison, the other set of specimens was naturally air-cooled (AC) at ambient temperature (22°C).

The tensile test specimens were produced from the bulk specimens after machining with the dimensions and geometry according to the drawings in Figure 2. Once machined to their final dimensions, a polishing silicon carbide paper of 800 grit was used to reduce the surface roughness.

Prior to the tensile tests, the specimens were annealed at two thirds of their respective melting temperature, for 16 hours. This moderate heat treatment relieved the stresses that were caused by the machining. As for the quenching procedure, tensile specimen preparation followed the NCMS recommendations [2].

The tensile tests were conducted using a computer-controlled MTS system, equipped with one-inch extensometers.

All the tensile tests were conducted with a cross-head speed of 0.01 in/min.

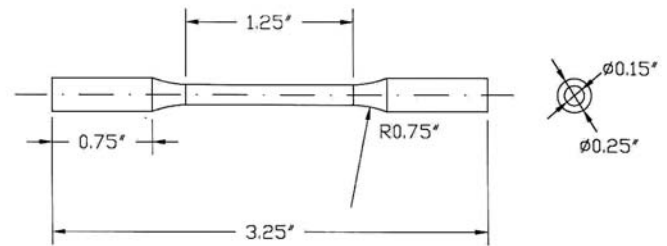


Figure 2. Geometric and dimensional configuration of the tensile test specimens.

Solder Droplets Production

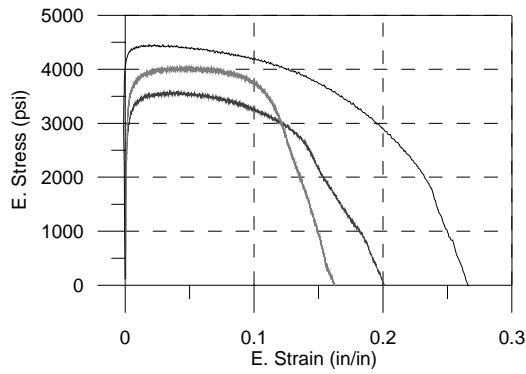
The solder droplets were produced under three different cooling rates. In this experiment the temperature was controlled by a copper plate where the molten solder was deposited. The temperature history was acquired using a thermocouple connected to a data acquisition system (DAS) and this to a computer. The three temperatures of the Cu plate were $T_1 = 0^\circ\text{C}$, $T_2 = 22^\circ\text{C}$ and $T_3 = 70^\circ\text{C}$.

RESULTS AND DISCUSSION

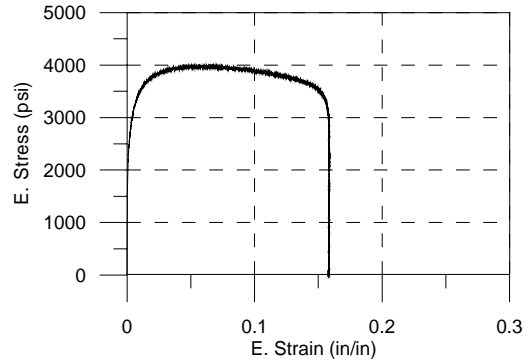
Tensile Testing

The results of the tensile testing for the three solder alloys are summarized in Figures 3 to 5. First, focusing on the tests conducted on the water-quenched specimens for the three alloys, the engineering stress-strain curves display some scatter, which was found to be caused by macroscopic defects, such as porosity, spread within the specimens. These defects resulted from casting and quenching. Nevertheless, the results were found to exhibit a range for the values of yield strength (YS), ultimate tensile strength (UTS), uniform and total elongation, which are shown in Table 1. Comparing the data for the three alloys it was determined that the ternary solder alloy, Sn-3.2Ag-0.8Cu, exhibited better mechanical properties than alloy Sn-3.5Ag and alloy Sn-0.7Cu, in that order [3].

For comparison, the air-cooled tensile test specimens were tested. For the case of the Sn-3.5Ag solder alloy, Figures 3 (a) and (b) clearly show that the mechanical behavior of the two types of specimens have similar properties in terms of YS and UTS. Similarly, for Sn-0.7Cu, Figures 4 (a) and (b) indicate a very good correlation of the tensile properties. In the same way, the two types of samples for Sn-3.2Ag-0.8Cu display almost equal tensile properties.

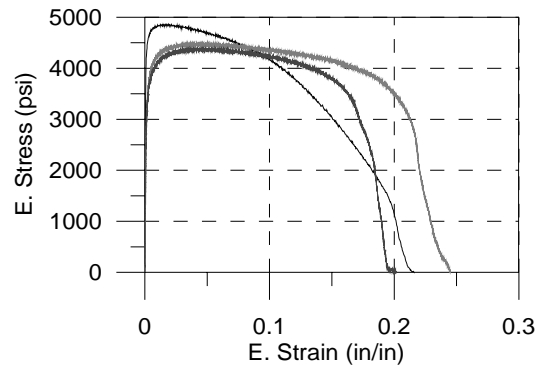


(a)

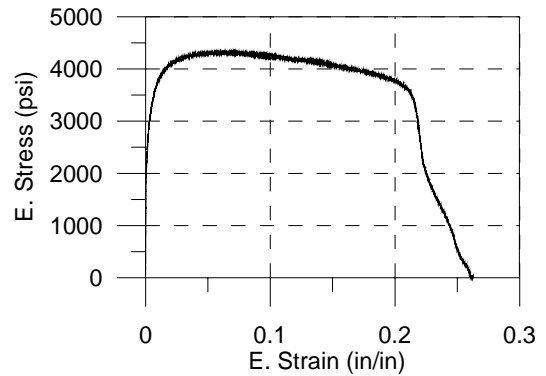


(b)

Figure 3. Engineering Stress – Strain curves for the Sn-3.5Ag specimens (a) water-quenched and (b) air-cooled.

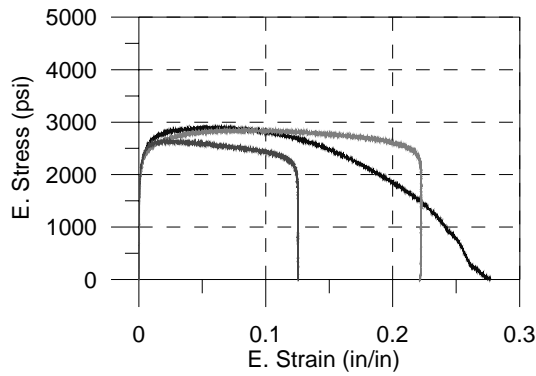


(a)

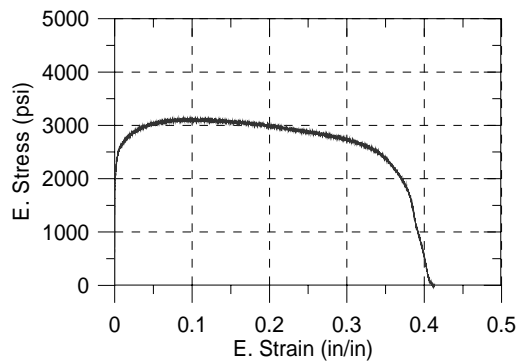


(b)

Figure 5. Engineering Stress – Strain curves for the Sn-3.2Ag-0.8Cu specimens (a) water-quenched and (b) air-cooled.



(a)



(b)

Figure 4. Engineering Stress – Strain curves for the Sn-0.7Cu specimens (a) water-quenched and (b) air-cooled.

Table 1. Summary of the tensile properties for bulk water-quenched and air-cooled specimens of alloys Sn-3.5Ag, Sn-0.7Cu and Sn-3.2Ag-0.8Cu.

Sample	Process	YS (psi)	UTS (psi)	Uniform Elongation (%)	Total Elongation (%)
Sn-3.5Ag	Q	4280	4450	2.9	26.3
Sn-3.5Ag	Q	2950	3580	4.3	20.1
Sn-3.5Ag	Q	3400	4040	5.0	16.2
AVG	Q	3540	4020	4.1	20.9
Sn-3.5Ag	AC	2730	4000	6.4	15.9
Sn-0.7Cu	Q	2200	2920	5.7	27.7
Sn-0.7Cu	Q	2180	2880	8.5	22.2
Sn-0.7Cu	Q	2290	2660	2.0	12.6
AVG	Q	2220	2820	5.4	20.8
Sn-0.7Cu	AC	2320	3130	9.1	41.2
Sn-3.2Ag-0.8Cu	Q	3770	4510	4.2	24.5
Sn-3.2Ag-0.8Cu	Q	4590	4860	1.9	21.6
Sn-3.2Ag-0.8Cu	Q	3610	4400	4.0	20.2
AVG	Q	3990	4590	3.4	22.1
Sn-3.2Ag-0.8Cu	AC	2880	4340	6.2	26.1

Solder droplets

As indicated previously, this set of experiments were conducted to determine the effects of cooling rate on the solder droplets for comparison with the tensile test specimens produced from the bulk solder samples. The information obtained from these experiments was the cooling curves [4] as illustrated in Figure 6. Here, the important features to note are the maximum temperature (T_{su}), that is the temperature at which the alloys were heated, the solidification temperature (T_{solid}), that is the temperature at which solidification occurs, the amount of undercooling ΔT , solidification time (t_s), and the cooling time after solidification to reach T_o (t_c). For this study, the cooling rate R , was defined as the slope of the curve right after solidification is completed.

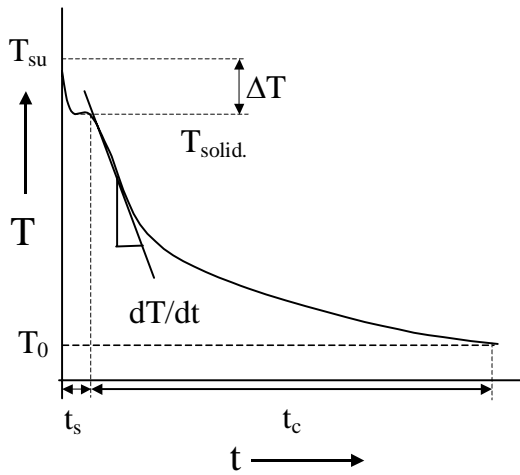


Figure 6. Schematic diagram of a cooling curve displaying the important features for data analysis.

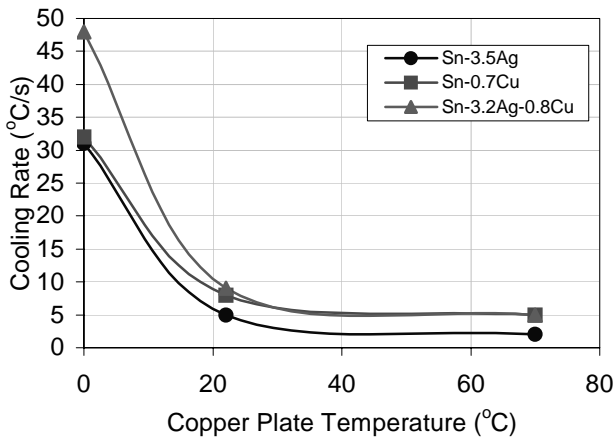
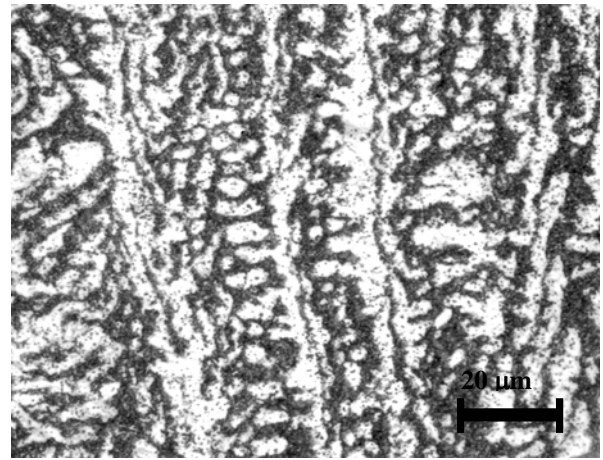
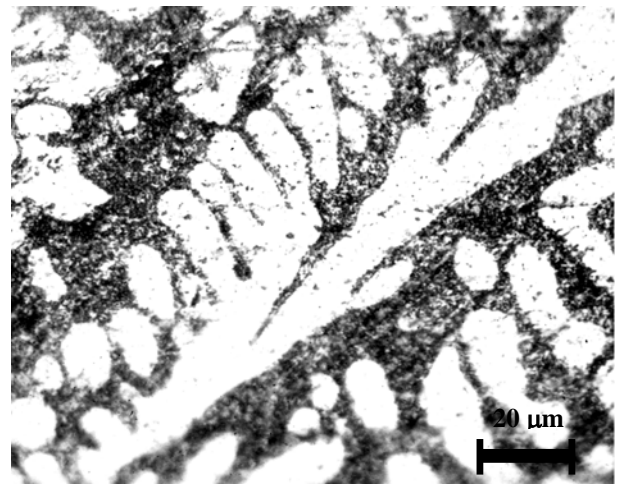


Figure 7. Different cooling rates produced by setting the initial copper plate temperature.

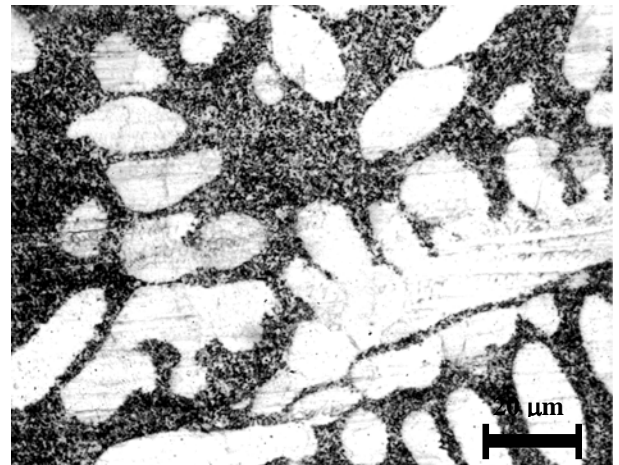
The effect of the copper plate temperature was clearly seen in the cooling curves. Fast cooling rates and short solidification times were obtained when the copper plate was set at the lowest



(a)



(b)



(c)

Figure 8. Effect of cooling rate on the microstructure of Sn-3.2Ag-0.8Cu solder alloy. (a) microstructure generated at $R = 48^\circ\text{C/s}$, (b) $R = 6^\circ\text{C/s}$, (c) $R = 5^\circ\text{C/s}$.

temperature ($T_1 = 0^\circ\text{C}$). As the set copper plate temperature increased, the cooling rate decreased (see Figure 7), and the cooling time to reach T_0 increased. Therefore, the three sets of specimens were indeed produced at three different cooling rates.

The effect of cooling rate on the microstructure of the solder droplets is clearly seen in the micrographs in Figure 8. These micrographs are for the ternary alloy Sn-3.2Ag-0.8Cu but are representative for the three alloys. They contain the features revealed in the three samples at the three different cooling rates. First, it was observed that the microstructure of all the solder droplets display a dendritic substructure [5]. Second, the difference was in the size of the dendrites, which increased as the cooling rate decreased.

The effect of the cooling rate on the size of the dendritic constituent was characterized by measuring the secondary dendrite arm spacing [6]. It was found that the cooling rate had a significant effect on the dendrite size. Figure 9 clearly shows that at slow cooling rates larger dendritic microstructures were produced. As the cooling rate increased the size of the dendrites decreased by a factor of three, which indicated that much finer solidification substructures were produced at high cooling rates.

In the case of the Sn-3.5Ag alloy, microstructural analysis revealed two microstructural phases, (1) dendrites of β -Sn and, (2) the eutectic interdendritic constituent consisting of Ag_3Sn [4]. In a similar manner, for the Sn-0.7Cu alloy, the microstructural constituents were found to be (1) dendrites of β -Sn and, (2) the eutectic interdendritic constituent consisting of Cu_6Sn_5 . For the ternary alloy Sn-3.2Ag-0.8Cu the microstructural phases present where (1) dendrites of β -Sn and, (2) the eutectic interdendritic constituent consisting of Ag_3Sn [7]. Very small amount of copper was found in solution mainly in the Ag_3Sn phase.

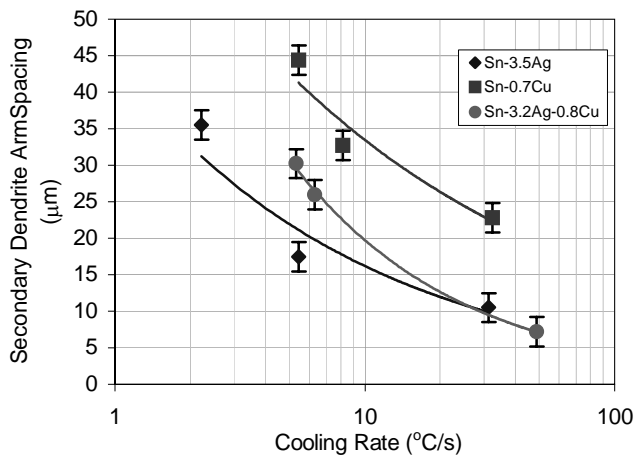


Figure 9. Variation of the secondary dendrite arm spacing as a function of cooling rate for the three solder alloys.

In all the cases the volume fraction of the phases varied as a function of cooling rate. The distribution of phases in the three alloys was found to exhibit similar behavior. For slow cooling

rates the volume fraction of the two phases was found to be near the predicted equilibrium volume fraction. However, as the cooling rate increased the interdendritic phase increased resulting in a decrease of the dendritic phase. What is important to note is that at high cooling rates, 48°C/s for Sn-3.2Ag-0.8Cu, the volume fraction of phases cannot be predicted from the respective equilibrium phase diagrams.

For the correlation of the specimens' microstructures with the mechanical properties, microhardness was measured. The correlation shown in Figure 10 indicates that hardness was lower on the coarser microstructures [4, 8], which were produced at lower cooling rates. As the secondary dendrite arm spacing decreased, thus indicating finer microstructures, the hardness increased.

Comparing the microstructures of the water-quenched tensile test specimens with those of the solder droplets in Figure 11, it was found to exhibit microstructures similar to those generated at slow cooling rates (Figure 7(c)), which also corresponds to those with low hardness values and consequently lower mechanical properties, see Figure 12.

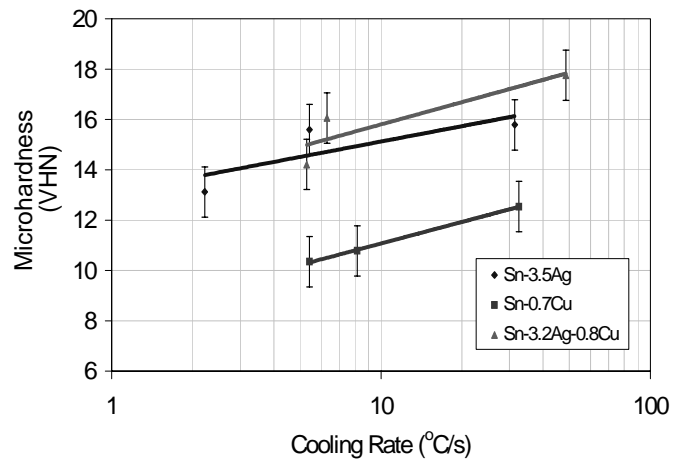


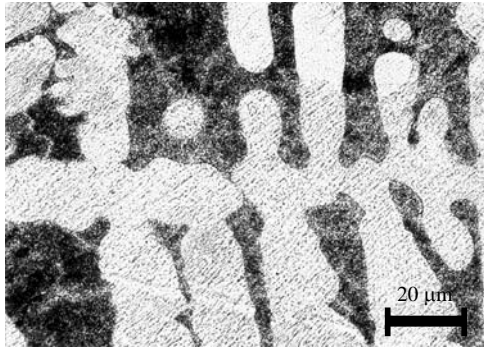
Figure 10. Relationship between the microhardness and the cooling rate for the three alloys.

The recommended procedure for the production of bulk solder samples consequently does not actually produce tensile testing specimens with microstructures similar to those found in actual solder joints. The difference can be even greater since as the technology advances, smaller electronic components are being developed and produced [9], the microstructure found in these solder joints are probably generated at faster cooling rates. Therefore, the mechanical property data collected must be for an equivalent microstructure to be useful for mathematical modeling of lifetime and reliability of solder joints.

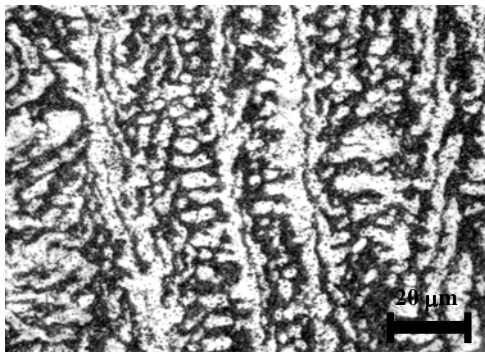
CONCLUSIONS

From the experiments and analysis discussed previously, the following conclusions can be drawn:

- The mechanical properties of both, the water-quenched and air-cooled tensile specimens were found to be similar.



(a)



(b)

Figure 11. Microstructures of the Sn-3.2Ag-0.8Cu solder alloy (a) water-quenched tensile testing specimen, (b) fast cooling rate solder droplet.

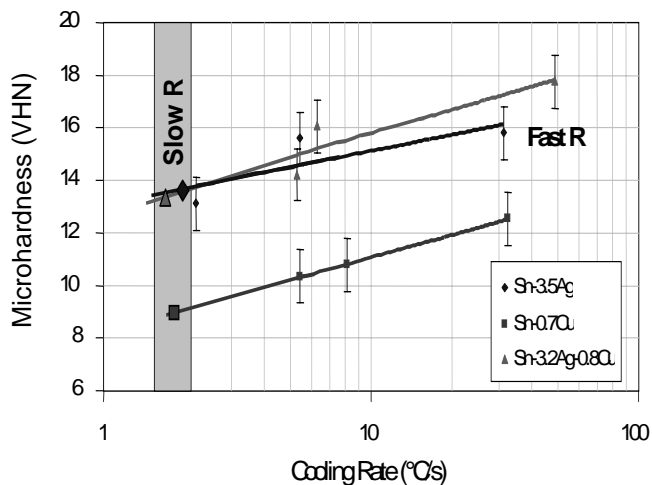


Figure 12. Microhardness measurements of the tensile testing specimens fall into the slow cooling rate zone.

- Alloy Sn-3.2Ag-0.8Cu exhibited higher strength and elongation at fracture than alloys Sn-3.5Ag and Sn0.7Cu, in that order.

- More importantly, the process of generating the bulk specimens for the production of tensile test specimens where found to exhibit slow cooling rate compared to the actual solder joints.
- These findings indicate that the procedure recommended by NCMS do not actually produce tensile test specimens that can be compared to the actual solder joints. Therefore, the mathematical models developed to predict the performance (lifetime and reliability) of joints based on these data may not compare well with the actual solder joint performance.

ACKNOWLEDGMENT

The authors are grateful to the Materials reliability Division of the National Institute of Standards and Technology for supporting this research.

REFERENCES

1. W. L. Winterbottom, "Converting to Lead-Free Solders: An Automotive Industry Perspective," *JOM*, pg. 20 – 24. July (1993)
2. "Lead-Free Solder Project," CD - report on the project by the National Center for Manufacturing Sciences, June (1998)
3. Li Xiao, Johan Liu, Songhe Lai, Lilei Ye, and Aders Tholen, "Characterization of Mechanical Properties of Bulk Lead-Free Solders," *2000 International Symposium on advanced Packaging Materials*, pg. 145 – 151, (2000)
4. S. Chada, A Herrmann, W. Laub, R. Fournelle, D. Shanguan and A. Achari, "Microstructural Investigation of Sn-Ag and Sn-Pb-Ag Solder Joints," *Soldering & Surface Mount Technology*, No. 26, pg. 9 – 13, 21, July (1997)
5. M. McCormack, G. W. Kammlott, H. S. Chen, and S. Jin, "New Lead-Free, Sn-Ag-Zn-Cu Solder Alloy With Improved Mechanical Properties," *Appl. Phys. Lett.* Vol. 65, No. 10, pg. 1233 – 1235, 5 September (1994)
6. M. C. Flemings, *Solidification Processing, Materials Science and Engineering Series*, p. 146-154, McGraw-Hill, (1974)
7. M. E. Loomans and M. E. Fine, "Tin-Silver-Copper Eutectic Temperature and Composition," *Metallurgical and Materials Transactions A*, Vol. 31A, pg. 1155 – 1162, April (2000)
8. M. R. Lambert, "Rapid Solidification of Lead-Based Solders," *Supplement to the Welding Journal*, pg. 215-s – 222-s, June (1989)
9. Dongkai Shanguan, Achyuta Achari, and Wells Green, "Application of Lead-Free Eutectic Sn-Ag Solder in No-Clean Thick Film Electronic Modules," *IEEE Transactions on Components, Packaging, and Manufacturing Technology – Part B*, Vol. 17, No. 4, pg. 603 – 611, November (1994).